Abellán-García, Joaquín; Torres-Castellanos, Nancy;
Fernández-Gómez, Jaime; Núñez-López, Andrés
Ultra-high-performance concrete with local high unburned carbon fly ash

Ultra-high-performance concrete with local high unburned carbon fly ash

Joaquín Abellán-García [a], Nancy Torres-Castellanos [b], Jaime Fernández-Gómez [c] & Andrés Núñez-López [d]

[a] Universidad Politécnica de Madrid, Madrid, Spain. Escuela Colombiana de Ingeniería Julio Garavito, School of Civil Engineering, Bogotá, Colombia. j.abellang@alumnos.upm.es
[b] Escuela Colombiana de Ingeniería Julio Garavito, School of Civil Engineering, Bogotá, Colombia. nancy.torres@escuelaing.edu.co
[c] Universidad Politécnica de Madrid, Department of Civil Engineering and Constructions, Madrid, Spain. jaime.fernandez.gomez@upm.es
[d] R&D, Cementos Argos SA, Medellín, Colombia. anunezn@argos.com.co

Abstract
Ultra-high-performance concrete (UHPC) is a kind of high-tech cementitious material with superb mechanical and durability properties compared to other types of concrete. However, due to the high content of cement and silica fume used, the cost and environmental impact of UHPC is considerably higher than conventional concrete. For this reason, several efforts around the world have been made to develop UHPC with greener and less expensive local pozzolans. This study aimed to design and produce UHPC using local fly ash available in Colombia. A numerical optimization, based on Design of Experiments (DoE) and multi-objective criteria, was performed to obtain a mixture with the proper flow and highest compressive strength, while simultaneously having the minimum content of cement. The results showed that, despite the low quality of local fly ashes in Colombia, compressive strength values of 150 MPa without any heat treatment can be achieved.

Keywords: ultra high-performance concrete (UHPC); high unburned carbon fly ash; optimization; sustainability; design of experiments (DoE).

Concreto de ultra alto desempeño con ceniza volante local con alto contenido de inquemados

Resumen
El concreto de ultra alto desempeño (UHPC) es un tipo de concreto de alta tecnología con excelentes propiedades mecánicas y de durabilidad en comparación con otros tipos de concreto. Sin embargo, debido al alto contenido de cemento y micro sílice necesarios, el costo y el impacto ambiental de UHPC es considerablemente mayor que el del concreto convencional. Por esta razón, se han realizado varios esfuerzos en todo el mundo para desarrollar UHPC con puzolanas locales más ecológicas y menos costosas. Este estudio tuvo como objetivo diseñar y producir UHPC utilizando cenizas volantes locales disponibles en Colombia. Por medio de una optimización numérica, basada en el diseño de experimentos (DoE) y criterios de optimización multiobjetivo, se obtuvo una mezcla con el flujo adecuado y elevada resistencia a la compresión, con las necesidades mínimas de contenido en cemento. Los resultados mostraron que, a pesar de la baja calidad de las cenizas volantes locales en Colombia, se pueden lograr valores de resistencia a la compresión de 150 MPa sin ningún tratamiento térmico.

Palabras clave: concreto de ultra alto desempeño (UHPC), ceniza volante con elevado contenido en inquemados, optimización, sostenibilidad, diseño de experimentos (DoE)

1. Introduction

Compared with ordinary cement concrete, ultra-high-performance concrete (UHPC) is normally characterized by the incorporation of micro-cementitious materials such as silica fume to improve particle compactness and pozzolanic reaction, combined with the use of superplasticizer to reduce the water-to-cementitious materials ratio [1–3]. These extremely low porosity and low permeability characteristics of ultra-high-performance concrete (UHPC) give it enhanced durability and mechanical properties over other types of concrete, such as normal concrete and high strength concrete
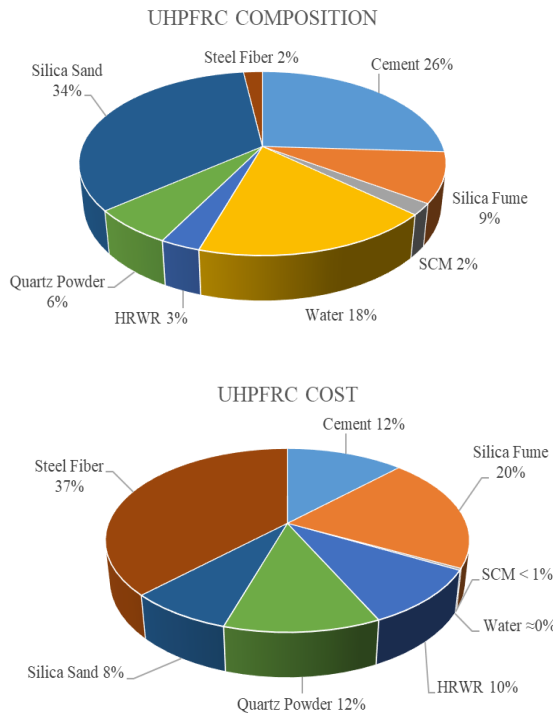
UHPFRC COMPOSITION

UHPFRC COST

Figure 1. Average dosage of 150 dosages from the scientific literature. Components and its implication in cost.
Source: The authors.

[1,4,5]. A typical UHPC mix contains Portland cement (CEM), silica fume (SF), quartz powder (QP), silica sand (SS) with a maximum size of 600 μm, high range water reduce superplasticizers (HRWR), and, possibly, steel fiber [6]. The fiber inclusion in UHPC improves the material's ductility, toughness, and tensile and flexural capacity [7]. In recent years, UHPC has been successfully applied to dam repairs, bridge deck overlays, coupling beams in high-rise buildings, the construction of footbridges, tunnel liner segments, and other specialized structure applications [8–12].

Abellan et al. [9] showed an average UHPC dosage of 150 dosages from scientific articles, sharing the following characteristics: compressive strength over 150 MPa without heat treatment, maximum size of aggregate between 0.5 and 0.6 mm, and 2% of steel fiber content in volume. This dosage and the cost implication of its components is shown in Fig.1.

The high quantity of cement in UHPC (over 800 kg/m^3) has a detrimental impact on sustainability [9,13,14]. In fact, Portland cement, the principal hydraulic binder used worldwide in modern concrete, is not only a product of an energy-intensive industry (4 GJ/ton of cement) but also responsible for large emissions of CO_2, thereby contributing to global warming [15]. Hence, one of the key sustainability challenges is to design and produce concrete with less clinker and inducing lower CO_2 emissions than a traditional one, while providing the similar mechanical properties, and better durability. UHPC seems to be one of the candidates to reduce the global warming impact of construction materials. This is because thinner sections can be made thanks to its excellent

mechanical behavior. However, when producing UHPC, the cement or binder content is always relatively high [16]. This is why the partial replacement of cement in UHPC, especially when made by locally available industrial by-products, is of great interest to the scientific community [17].

Fly ash (FA) is a by-product from furnaces fired with pulverized coal, often power-plants. It consists of spherical particles as shown in Fig. 2c. Fly ash can be either an aluminosilicate or a calcium silicate, and because of the reactive silicon dioxide (SiO_2) that both types contain, fly ash has pozzolanic properties [18,19]. The American Society for Testing and Materials (ASTM) established two classes of fly ash, Class F from bituminous coal and Class C from subbituminous and lignite coal [20]. As noted from the ASTM specification, one difference between Class C and F fly ashes is the minimum limit of 50% for the combination of SiO_2, Al_2O_3, and Fe_2O_3 for Class C and 70% for Class F. The level of unburned carbon or organic matter expressed as its loss of ignition (LOI) limit is a maximum of 6% for Class C and 12% for Class F. However, the use of Class F pozzolan containing up to 12% loss on ignition could be approved if either acceptable performance records or laboratory test results are made available. It should be stressed that FA pozzolanic activity mainly depends on the glassy phase type and amount, mineral component fineness, particle morphology, and LOI [21]. Regarding fineness, a maximum threshold of 34% amount retained on 45 μm (No. 325) sieve is also established [20].

FA is one of the most successfully used supplementary cementitious material in partial replacement of cement in UHPC [18]. It is usually combined with ground granulated blast slag furnace (GGBFS), SF and/or steel slag powder (SS), etc., as a binary, ternary or quaternary system [18]. Yazici et al. [22] found that the compressive strength of UHPC containing a high content of FA (LOI 1.30%) and GGBFS reached over 200 MPa after standard room curing, 234 MPa after steam curing, and 250 MPa after autoclave curing. The combination of GGBFS and fly ash can enhance flexural strength, and significantly improve the toughness of concrete after all curing regimes [22]. However, it decreased the modulus of elasticity of UHPC, especially with more than 30% replacement of cement. Ferdosian et al. [23] proved that incorporating FA in UHPC as a partial substitution of cement and silica fume could lead to a more sustainable concrete which reaches the threshold values in flowability and compressive strength when replacing a 16% in weight of cement. Furthermore, if the substitution were made by ultra-fine fly ash (UFFA) with d_{50}=4.48μm, the percentage could reach 20% without compromising the compressive strength of UHPC. The FA used in this research had a LOI value of 3.00%. The effect of a different dosage of FA (LOI =0.30%) on the compressive strength, flexural strength, and fracture toughness were analyzed by Chen et al. under different autoclaving conditions [24]. The results showed that the addition of 10–30% fly ash increased compressive and flexural strength of UHPC after both standard curing and suitable autoclave curing. The autoclave curing effectively improved the compressive and flexural strength of UHPC, with the maximum increase of 37.5% and 30.3% respectively. As more fly ash was added, a higher pressure of

autoclave curing was needed for the UHPC to obtain the highest strength [24].

However, the use of low-quality local available FA in Colombia, with the loss of ignition values over 12%, as a component of UHPC is an open question.

Towards a cost-effective and more sustainable UHPC, the objective of this study is to effectively design and produce UHPC with low cement amounts, a maximum content of silica fume of 100 kg/m^3, using micro limestone powder and high unburned carbon local FA as a cementitious supplementary material. The design of the concrete mixtures is based on the goal of achieving mechanical and rheological properties with minimum amounts of cement through a 3-factor Design of Experiments (DoE). To ensure a densely compacted cementitious matrix, the modified Andreasen & Andersen particle packing model ($A\&A_{mod}$) [25] was used.

With the concept of DoE, we use a set of well-chosen experiments which must be carried out by the researcher. The purpose of this design is to optimize a process or system by performing each trial and to draw conclusions about the significant behavior of the studied object from the results of the trials. Considering the costs of a single experiment, minimizing the amount of performed experiments is always a goal. With DoE, this number is carried on being as low as possible and the most informative combination of the factors is selected. Therefore, DoE is an effective and cost-effective solution [1,26,27].

On the other hand, response Surface Methodology (RSM) is a statistical tool for the analysis of problems in which a response is affected by several factors [4,26,28,29]. This method has been widely used for experimental process optimization in UHPC research [1,30].

In this study, a multi-objective simultaneous optimization R-coded algorithm [31] was employed, pointing to determine the optimum value of the DoE's factors that derive in a proper flow with the maximum compressive strength (exceeding 150 MPa) and a minimum amount of cement possible when using local FA in tis composition. Eventually, the goodness of the mathematical model was evaluated through the comparison with experimental work results.

2. Local fly ash in Colombia

2.1 Coal thermoelectric production

According to Fonseca-Barrera [32] coal thermoelectric production in Colombia is concentrated mainly in the departments of La Guajira and Cesar, with more than 90% of national production, which is mostly exported, while the rest is produced in departments such as Boyacá, Norte de Santander, Cundinamarca, Antioquia and the Valle del Cauca. The production of these departments is destined to satisfy the internal consumption of coal.

The departments of Boyacá and Norte de Santander are the main producers of metallurgical coal destined to the national market, exporting only one third of the production.

Likewise, the production of energy in thermoelectric plants bases its operation on the consumption of mineral coal which, through technological processes, is subjected to combustion where energy is released in the form of heat that is used for the production of water vapor. This steam is directed into a turbine that takes its energy and converts it into electrical energy through a generator.

Currently, there are four thermoelectric plants in the country, operated by the companies Emgesa S.A. E.S.P., Energy Management S.A. E.S.P., Termo-Sochagota E.S.P. and Termotasajero SA, which are located in the municipalities of Tocancipá, Paipa, Paipa, and Cúcuta respectively, which have been in operation for 48 years with the installation of Paipa-1 and the most recent, with 16 years of operation, is Paipa-4 [32].

The net effective capacity is 700 MW. Tocancipá contributes 32%, Paipa 46%, and Cucuta the remaining 22%. The technology used in the three plants is conventional pulverized coal [32].

2.2 Local fly ash

Several efforts were made in the scientific community in Colombia to study the effect of local FA as a cementitious supplementary material. Valderrama et al. [33] evaluated the mechanical performance and durability of concretes with local type F fly ash (LOI: 10.68%). The authors observed that the resistance increases with the age of curing, however, at early ages (below 28 days) the specimens added with ash present a lower resistance to the standard sample (0% addition), indicating low reactivity. Fonseca-Barrera [32] compared three different sources of local FA in Colombia: Termopaipa, Termo-Sochagota, and Termotasajero. The research involved concrete's mechanical properties and durability. The results concluded that variability and lack of controls in production and management of Colombian FA, does not provide adequate conditions to improve the durability properties against chloride ion attack.

In this study, a local high unburned carbon fly ash from Termotasajero was used. Its chemical analysis can be observed in Table 1.

3. Experimental investigation

3.1 Materials

The materials used to produce the concrete were locally available in Colombia. ASM Type HE cement was employed. HE cement had a specific gravity of 3.15, and mean particle diameter (d_{50}) of 8 μm. The silica fume employed in the experimental campaign complied with ASTM C-1240 specifications. Silica fume had a specific gravity of 2.20 and d50 of 0.15 μm. The concrete was also designed with a silica sand of a specific gravity of 2.65, maximum particle size (d_{max}) of 600 μm, and d_{50} of 165 μm. The locally available FA with a specific gravity of 2.32 and d50 of 30 μm was also employed. Finally, micro-limestone powder with a specific gravity of 2.73 and d_{50} of 2 μm was used as supplementary cementitious materials. Table 1 shows the chemical composition of the materials used in this study. The supplementary cementitious materials utilized were studied by scanning electron microscopy (SEM) as showed in Fig. 2. Results indicated the spherical shape of the FA and SF particles, and the small size of the latter.
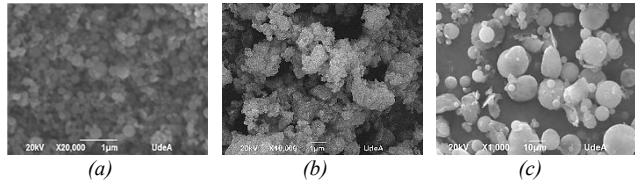
Figure 2. FSEM of supplementary cementitious materials used in research: *(a)* silica fume; (b) Limestone powder; and *(c)* locally available fly ash.
Source: The authors.

Table 1.
Chemical properties of materials.

| Chemical analysis	Cement	SF	LP	FA	SS
SiO_2%	19.42	92.29	0.90	50.09	95.80
Al_2O_3%	4.00	0.59	0.10	22.26	0.11
CaO%	64.42	3.89	55.51	2.19	0.38
MgO%	1.52	0.26	0.70	0.53	0.20
SO_3%	1.93	0.07	0.10	0.03	0.52
Na_2O%	0.19	0.31	0.03	0.31	0.25
K_2O%	0.39	0.54	0.00	0.99	3.49
TiO_2%	0.38	0.01	0.00	1.05	0.25
Mn_3O_4%	0.05	0.01	0.01	0.01	0.01
Fe_2O_3%	3.61	0.24	0.05	11.54	0.09
Loss of ignition %	2.58	0.60	42.21	12.45	0.31
Specific gravity (gr/cm³)	3.16	2.20	2.73	2.32	2.65

Source: The authors.
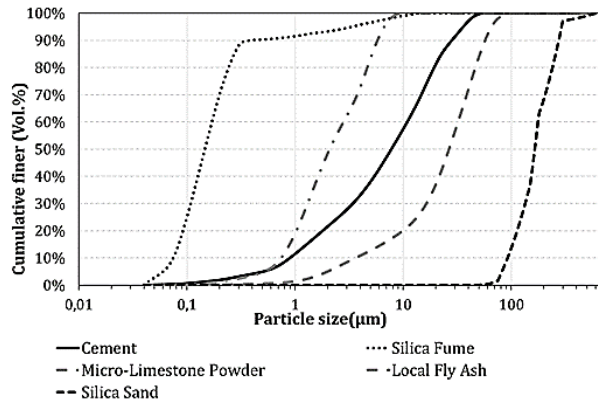
Figure 3. Particle size distribution of the used materials.
Source: The authors.

Fig. 3 provides the particle size distribution (PSD) of the cement, silica fume, micro-limestone powder, local fly ash and SS. A polycarboxylate (PCE)-based HRWR with a SG of 1.07 and solid content of 40% was used as a superplasticizer.

3.2 Specimens

The design of each dosage required several steps. The amounts of cement, water and superplasticizer were determined by the DoE. The other components were ruled by the *A&A*$_{mod}$ using a *q* value of 0.264, according to Eq. (1).

$$P(D) = \frac{\left(D^q - D_{min}^q\right)}{\left(D_{max}^q - D_{min}^q\right)} \qquad (1)$$
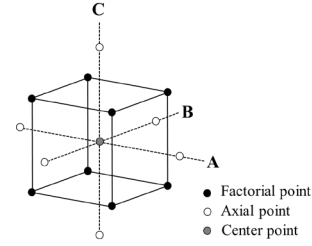

Figure 4. Central Composite Design for 3 design variables at 2 levels
Source: The authors.

Table 2.
Independent variables and range of variation.

Factor	Coded	Range of variation				
		-1.789	-1	0	1	1.789
Cement (kg/m³)	A	566.334	590.000	625.000	650.000	673.666
w/b	B	0.156	0.16	0.165	0.17	0.174
HRWR(%vol)	C	1.842	2	2.2	2.4	2.556

Source: The authors.

where *D* is the particle size, *P(D)* is the weight fraction of total solids that are smaller than *D*, D_{max} and D_{min} are the maximum and minimum particle sizes, respectively, and q is the Fuller exponent. The value of *q* was determined in previous research [4].

Central composite design (CCD) is the most used response surface designed experiment. In this study a three factor (i.e. cement content, w/b, and HRWR content) central composite, as depicted in Fig. 4, was used. For further information about CCD please refer to [1,30].

The statistical analysis was performed on the coded data sets in order to simplify the interpretation of the results. The coding was according to Eq. (2):

$$X_j = \frac{(Z_j - Z_{0j})}{Z_{max} - Z_{min}} \qquad (2)$$

where X_j is the coded factor level, Z_j is the real value of the factor, Z_{0j} is the real value of the factor at the center point, and Z_{max} - Z_{min} represents the difference between the maximum and the minimum values of the factor considered in the factorial design.

After performing the experiments, a second-degree polynomial equation was used to estimate the responses [34], according to Eq. (3) in the form of:

$$R = a_0 + \sum a_i x_i + \sum a_{ii} x_i^2 + \sum a_{ij} x_i x_j \qquad (3)$$

where R is the estimate of the response variable, a0 is the interception or overall mean response, ai represent the linear coefficients, aii represent the second-order coefficients, aij represent the coefficients of the interaction, and xi, xj are the selected factors. The factors defined for this experiment and their control levels are depicted in Table 2.

To summarize, an 18-set-point central composite design, considering three independent factors, was performed. The corresponding mixture proportions of this DoE, adjusted according to the A&Amod curve, are presented in Table 3.

Table 3.
Proportion of mix components expressed as a function of the weight of cement.

Run	C	SF	EASF	GPF	MLP	PCE	SS	w/b
1	1	0.167	0.625	0.117	0.083	0.036	1.552	0.160
2	1	0.154	0.492	0.069	0.077	0.033	1.510	0.160
3	1	0.167	0.625	0.117	0.083	0.036	1.499	0.180
4	1	0.154	0.492	0.069	0.077	0.033	1.463	0.180
5	1	0.167	0.625	0.117	0.083	0.043	1.548	0.160
6	1	0.154	0.492	0.069	0.077	0.040	1.506	0.160
7	1	0.167	0.625	0.075	0.083	0.043	1.553	0.180
8	1	0.154	0.492	0.069	0.077	0.040	1.459	0.180
9	1	0.160	0.540	0.084	0.080	0.038	1.539	0.170
10	1	0.160	0.540	0.084	0.080	0.038	1.539	0.170
11	1	0.172	0.646	0.121	0.086	0.041	1.625	0.170
12	1	0.149	0.449	0.075	0.075	0.035	1.434	0.170
13	1	0.160	0.540	0.084	0.080	0.038	1.583	0.150
14	1	0.160	0.540	0.084	0.080	0.038	1.495	0.190
15	1	0.160	0.540	0.084	0.080	0.032	1.543	0.170
16	1	0.160	0.540	0.084	0.080	0.044	1.535	0.170
17	1	0.160	0.540	0.084	0.080	0.038	1.539	0.170
18	1	0.160	0.540	0.084	0.080	0.038	1.539	0.170

Source: The authors.

Table 4.
The set point combinations and the corresponding experimental responses.

Run	A	B	C	$\varnothing_m$ (mm)	R28 (MPa)
1	-1	-1	-1	220.00	124.20
2	1	-1	-1	216.75	133.58
3	-1	1	-1	260.75	115.28
4	1	1	-1	256.00	128.23
5	-1	-1	1	262.00	132.65
6	1	-1	1	255.75	142.25
7	-1	1	1	280.00	124.57
8	1	1	1	274.75	129.44
9	0	0	0	261.75	128.19
10	0	0	0	264.25	127.64
11	-1.789	0	0	264.25	129.45
12	1.789	0	0	244.50	144.31
13	0	-1.789	0	209.50	138.51
14	0	1.789	0	273.00	125.57
15	0	0	-1.789	243.00	115.25
16	0	0	1.789	271.75	138,86
17	0	0	0	270.25	130.71
18	0	0	0	269.50	129.59

Source: The authors.

3.3 Items of investigation

In preparing specimens, a 5-liter mortar type laboratory mixer was used. At the end of the mixing, tests were conducted, still in a fresh state, to determine static slump flow diameter in accordance with ASTM 1437 specifications [35]. The slump cone is filled with UHPC, the cone lifted, and the spread of the concrete measured, without dropping the table. The spread diameter of the mortar was measured in four perpendicular directions, and the average of the diameters was reported as the spread flow of the concrete ($\varnothing$m) in mm, according to Eq. 4.

$$\varnothing_m = \frac{1}{4} \sum_{i=1}^{4} \varnothing_i \qquad (4)$$

After preforming the workability test, the UHPC was cast in molds and compacted on a vibrating table. The prisms were demolded approximately 24 h after casting and then cured in a moisture room at 95% of relative humidity and 20 ºC until the day of the test, without any heat treatment applied. For the determination of the compressive strength, cubes of 50 mm were tested. A compression testing machine with a capacity of 3000 kN was used, following ASTM C109 [36]. Three samples were tested for each of the following ages: 24 hours, 7 days and 28 days.

To summarize, three factors were chosen, namely cement content in kg/m³ – coded as factor A -, water to binder ratio (w/b)- coded as factor B -, and the volume of superplasticizer to the total dosage ratio (HRWR) -coded as factor C-. To define the proportion of the other components of the concrete, the $A\&A_{mod}$ curve was employed. Two responses were also considered, encompassing compressive strength without special curing conditions at 28 days (R28), and spread flow ($\varnothing_m$).

4. Experimental results

Table 4 shows the set point combinations defined in the CCD and their corresponding experimental response values.

Table 5.
Results for developed regression models for response Øm

Model Terms	$\varnothing_m$	
	Coeff	P-value
Inter.	249.638	<0.0001
A	-3.808	0.0500
B	16.044	<0.0001
C	11.812	<0.0001
A:B	-	-
A:C	-	-
B:C	-5.375	0.0416
A:B:C	-	-
A^2	-	-
B^2	-6.415	0.0019
C^2	-	-

Source: The authors.

R, a language and environment for statistical computing, experiment design, and analysis, was used to plan the experiment.

4.1 Model adjusting and validation

For each response (R28, and $\varnothing_m$) a quadratic polynomial regression model based on Eq. (3) was fitted from the DoE design data. The process is then followed by removing the variable with the largest p-value. The procedure continues until only those variables which are significant (p-value<0.05) remain in the model. After removing each term, the fitting process is repeated until all the non-significant terms have been removed from the model. To investigate the significance of the model, an analysis of variance (ANOVA) was performed using R [37]. The results analysis for full regression models included the determination coefficient (R^2), the adjusted coefficient of multiple determinations (Adj-R^2), the root mean squared error (RMSE), the F Statistic value, the lack-of-fit p-value, and the model p-value. After the model was created, the next step was to verify its efficiency by performing the residual analysis. The latter involves statistical calculation such as residual standard deviation as well as residual plots, in which the adequacy of

the selected model can be graphically evaluated. Finally, a comparison of the predicted and real values was depicted. If the test demonstrates an adequate model, the response surface counter can be plotted [29].

4.2 Slump flow

The coefficients of the model (estimation parameter) and the corresponding P-values are presented in Table 5.

The p-value for all the variables which remain in the model after the backward elimination procedure is lower than 0.05. This indicates their significance in the model.

Table 6 shows the results of the analysis of variance (ANOVA) performed in order to investigate the significance of the model for response average slump flow ($\varnothing_m$). A p-value lower than 0.0001 was obtained for the model, implying that the model is significant. The model presented a high determination coefficient (R^2) explaining 92.8% of the variability in the response $\varnothing_m$. This indicates the goodness of fit for the model and high statistical significance of the model. Furthermore, the adjusted R^2 value is very close to the R^2 which shows that the unnecessary terms are not added in the model. The accuracy of the model was evaluated by performing a lack-of-fit test. A non-significant lack-of-fit indicates an accurate model. The p-value obtained by ANOVA implied that the lack-of-fit is not significant compared to the pure-error sum of squares.

Fig. 5a shows the normal probability plot of the residuals of the $\varnothing_m$-model. The residuals lie reasonably close to a straight line, implying that errors are distributed normally and supporting the claim that the terms mentioned in the model are significant.

A graph of the predicted response values versus the actual response values is depicted in Fig. 5b. It shows the high correlation between the experimental and predicted values. These high values of correlation coefficient validate the adequacy of the model used to navigate the design space.

Table 6.
Results for developed regression models for response $\varnothing_m$.

Response	R^2	Adj-R^2	RMSE	F-Stat	Lack of fit	P-value
$\varnothing_m$	0.928	0.898	5.442	30.892	6.666	<0.0001

Source: The authors.

Table 7.
Results for developed regression models for response R28

Model Terms	R28	
	Coeff	P-value
Inter.	124.221	<0.0001
A	4.384	0.0001
B	-4.053	0.0003
C	4.841	<0.0001
A:B	-	-
A:C	-	-
B:C	-	-
A:B:C	-	-
A²	2.090	0.0163
B²	-	-
C²	-	-

Source: The authors.

Table 8
Results for developed regression models for response R28

Response	R^2	Adj-R^2	RMSE	F-Stat	Lack of fit	P-value
R28	0.879	0.842	2.664	23.611	3.134	<0.0001

Source: The authors.

4.3 Compressive strength

The coefficients of the fitted model for response 28-day compressive strength and its corresponding p-values are depicted in Table 7.

The p-value for all the variables which remain in the model after the backward elimination procedure is lower than 0.05.

Table 8 shows the results of the analysis of variance (ANOVA) performed to examine the significance of the model for response 28-day compressive strength (R28). A model p-value lower than 0.0001 determined that the model is significant. Furthermore, the model showed a high R^2 value explaining 87.9% of the variability in the response R28. The Adjusted R^2 value is very close to the R^2, determining that the unnecessary terms are not included in the model. Also, the analysis presents a non-significant lack-of-fit.

A normal probability plot of the residuals of R28-model is depicted in Fig. 6a. The residuals lie reasonably close to a straight line, implying that errors are distributed normally, supporting the claim that the terms mentioned in the model are significant.

Fig. 6b shows the model's predicted values versus the experimental values. It shows the high correlation between the experimental and predicted values. These high values of correlation coefficient validate the adequacy of the model used to navigate the design space.

Figure 5. Normal Plot of residuals (a) and Predicted versus Actual values (b) for a fitted model for $\varnothing_m$.
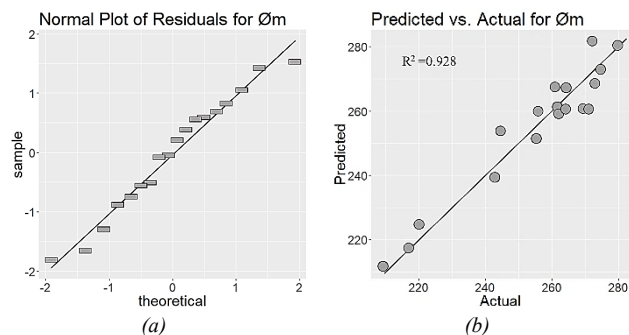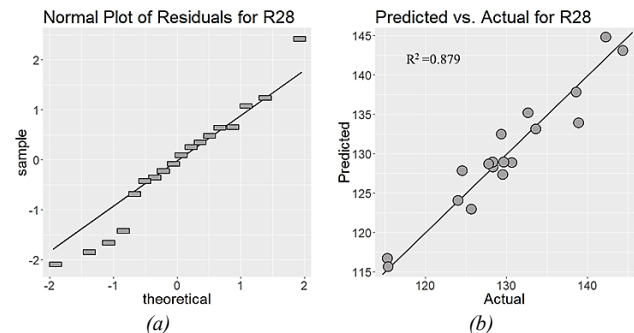Source: The authors.

Figure 6. Normal Plot of residuals (a) and Predicted versus Actual values (b) for a fitted model for R28.
Source: The authors.

5. Factor analysis using response surface methods (RSM)

After the model was evaluated, the effect of each factor and their interactions on the response was investigated. RSM plots were established as a simple interpretation of the derived statistical models. The RSM plots were used to compare the trade-off between the effects of factors B and C (i.e. w/b and HRWRA, respectively) on the considered responses. For each response, three graphs were plotted, corresponding to the factor points and the central one for factor A. This means one contour plot for A=-1, i.e. cement content of 590 kg/m³, another graph for A=0, i.e. cement content of 620 kg/m³, and the last one for A=1, i.e. cement content of 650 kg/m³. These plots provide information on the effect of the three factors and their interactions on average spread ($\emptyset_m$) and compressive strength with standard curing conditions at 28 days (R28).

5.1 Slump flow

Fig. 7 depicts the RSM plots for $\emptyset_m$ response, for different fixed values for Cement content.

According to the polynomial-model, presented in Table 5, a non-linear relation was obtained between the spread length and the water to binder ratio, which is the most significant factor. Complying with EFNARC [38], a spread flow value from 240 to 260 mm is considered adequate for a plain SCC mixture. The consequence of the reduction of cement (d_{50}=8μm) is a higher amount of local fly ash (d_{50}=30 μm) and micro limestone powder (d_{50}=2.1 μm), due to adjusting the mix to the $A\&A_{mod}$ curve. Using limestone powder as a cement replacement to produce UHPC can significantly improve its workability [16]. On the other hand, FA, thanks to its larger particle size and spherical shape, interrupts the formation of flocs and acts as a plasticizer or lubricant [39,40]. Hence, the more fly ash and limestone particles and the less cement content (factor A) there are, the higher the value of spread flow. As expected, the water to binder ratio (factor B) and superplasticizer content (factor C) have a positive effect on the spread flow value. The water to binder ratio has a higher influence in this field.
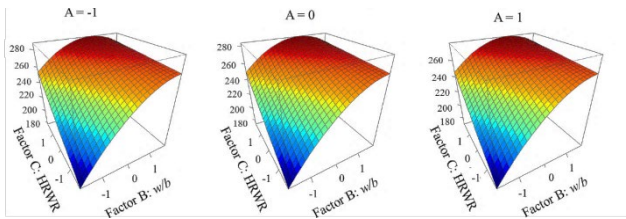

Figure 7. Contour plots to compare the trade-off between the effects of B and C on $\emptyset_m$ response, for different fixed values of factor A.
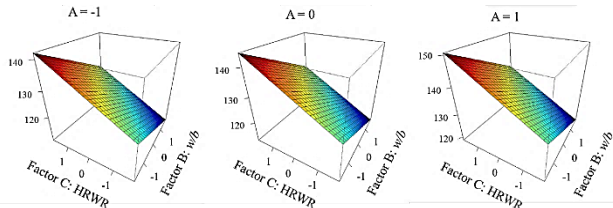Source: The authors.

Figure 8. Response surface 3D plots indicating the interaction effects of w/b ratio (B) and superplasticizer content (C) on the 28-day compressive strength. The cement content was fixed at 625 kg/m³ (A=0).
Source: The authors.

5.2 Compressive strength

Fig. 8 depicts the RSM plots for 28-day compressive strength response, for different fixed values for factor A.

Factor A has the most significance regarding compressive strength. The more cement there was in the dosage, the less fly ash and micro-limestone powder due to the $A\&A_{mod}$ curve. The fly ash could have a negative effect on the compressive strength because of the high unburned carbon content. As shown in Fig. 8, Factor C also has a positive effect on the 28-day compressive strength of UHPC. However, Factor B has an adverse effect on 28-day compressive strength.

6. Multi-objective optimization

6.1 Methodology

A multi-objective optimization R-coded algorithm [31] was employed, aimed at settling the optimum values for the factors of the design that can reach the best value for the response. Once the second-order regression models between factors and responses were selected, all factors were randomly assigned simultaneously and independently to enhance the best trade-off of the objective functions without excessively compromising any of the requirements [26,41].

The optimization R-coded algorithm used in this study was based on the desirabilities approach developed by Derringer & Suich [42], where the predicted values of each response variables are transformed into values within the interval [0,1] using three different desirability methods for the three different optimization criteria (i.e. minimize, maximize, in range). Each value of a response variable can be assigned a specific desirability, optimizing more than one response variable.

Derringer & Suich [42] defined the desirability cases of minimization, maximization, and in range individual responses, as in Eqs. (5), (6) and (7), respectively.

$$d = \begin{cases} 1 & Y_i \leq L \\ \left[\dfrac{U - Y_i}{U - L}\right]^{wt_i} & L < Y_i < U \\ 0 & Y_i \geq U \end{cases} \quad (5)$$

$$d = \begin{cases} 0 & Y_i \leq L \\ \left[\dfrac{Y_i - L}{U - L}\right]^{wt_i} & L < Y_i < U \\ 1 & Y_i \geq U \end{cases} \quad (6)$$

$$d = \begin{cases} 0 & Y_i \leq L \\ 1 & L < Y_i < U \\ 0 & Y_i \geq U \end{cases} \quad (7)$$

The most widely used method to draw the optimal solution is to optimize by converting multiple desirability functions into single desirability D [42]. The geometric mean of the specific desirabilities characterizes the overall desirability as follows in Eq. (8):

$$D = (d_1^{r_1} \times d_2^{r_2} \times d_3^{r_3} \times \ldots \times d_n^{r_n})^{1/\Sigma r_i} = \left[\prod_{i=1}^{n} d_i^{r_n}\right]^{1/\Sigma r_i} \quad (8)$$

Table 9.
Optimization of the individual responses for a self-compacting UHPC mixture with high 28 days compressive strength (Criteria I) and with minimum cement content (Criteria II).

Responses and variables	Lower	Upper	Goal
$Ø_m$(mm)	240	260	In range
R28(MPa)	150	165	Maximum
C(kg/m^3)	600	650	Minimum

Source: The authors.

Table10.
Optimum mixture.

Mix		A	B	C	Desirability
Criteria I	Coded	1.19	-0.149	1.7889	0.928
	Real	654.81	0.164	0.0256	
Criteria II	Coded	-0.149	-0.149	1.7889	0.675
	Real	621.27	0.164	0.0256	

Source: The authors.

A value of D different from zero in Eq. (8) implies that all responses are in a desirable range simultaneously and, consequently, for a value of D near 1, the combination of the different criteria is globally optimum, so the response values are close to their target values. However, if any of the responses fall outside their desirability range, the overall function becomes zero. In Eq. (8), r_i represents the relative importance assigned to the response i. The relative importance ri is a comparative scale for weighting each individual desirability functions (d_i) in the overall desirability product and it varies from the least important ($r_i = 1$) to the most important ($r_i = 5$). It is important to denote that the outcome of the overall desirability D depends on the r_i value that offers users flexibility in the definition of desirability functions. In this study, shape constants are equal to 5 in all cases.

The goals of the criteria optimization for each response are shown in Table 9. It has been proposed to select the optimum mix design variables for obtaining a self-compacting mixture according to EFNARC criteria [38] with the maximum 28-days compressive strength and the minimum content of cement. In this regard, the slump flow was defined as 'in range' goal, while 28-day compressive strength was defined as the 'maximum' goal, and the cement content was defined as 'minimum' goal. At the end of the multi-objective optimization process, one optimal solution satisfying the specified constraints was obtained. The optimized mixture is presented in Table 10.

6.2 Validation of the multi-objective optimization

The efficiency of the designed model was evaluated by carrying out the experiment with the selected value of factors and by comparing experimental measured values obtained with those indicated by the mathematical model. Mixture selected by the multi-objective algorithm is presented in Table 10. The comparison between theoretical and experimental results is shown in Table 11. The percentual deviation was employed as a measure of accuracy for validation. Results confirmed that the experimental values agree with the values predicted by the proposed model.

Table11.
Forecast responses by model versus experimental values

$Ø_m$(mm)		Deviation (%)	R28 (MPa)		Deviation (%)
Experimental	Model		Experimental	Model	
245.50	250.83	2.12%	151.78	157.55	3.66%

7. Discussion

To reach a compressive strength of 150 MPa an amount of 703 kg/m^3 of cement was needed. This does not represent an excessive reduction in the cement content compared to the average dosage shown by Abellan et al. [9], even more so if we take into account that MLP was also used in the binder.

As mentioned, FA is one of the most successful supplementary cementitious materials used in the partial replacement of cement in UHPC. Several researches have demonstrated its potential as a high-volume partial substitution of cement in UHPC with fine silica sand as aggregate (0.5-0.6 mm), achieving the compressive resistance threshold with only 500-575 kg of cement by m^3 [43–45]. However, FA used in those studies did not reach to the 3% LOI.

8. Conclusions

In this research, local high unburned carbon fly ash was evaluated as supplementary cementitious material in UHPC mixture. Using a multi-objective simultaneous optimization algorithm, a cost-effective and eco-friendly ultra-high-performance concrete using local high unburned carbon fly ash and micro limestone powder as a partial substitution of cement and silica fume was obtained. Three factors: spread flow, compressive strength at 28 days, and cement content, were studied and used in the multi-objective simultaneous optimization algorithm. Based on the results of this experimental investigation, the following conclusions were drawn:

An optimal mixture using local high unburned carbon fly ash was designed to reach 150 MPa at 28-day compressive strength with 703 kg/m^3 of cement and 100 kg/m^3 of silica fume, in addition to micro limestone powder.

The proposed RSM-mathematical model provides a good prediction of UHPC properties over the chosen range of cement content, water to binder ratio and superplasticizer content. The low values of lack-of-fit test results in addition to high values R^2, demonstrated the accuracy of the second-order models to predict performance of UHPC, in relation to compressive strength at 28 days, as well as spread flow value. The ANOVA test also verified that no unnecessary terms were included into the models.

A multi-objective simultaneous optimization algorithm was also useful, with the intent of obtaining an eco-friendly mixture with maximum compressive strength, and, simultaneously, with the minimum amount of cement content.

The high content of unburned carbon makes it difficult to achieve greater substitution of cement using local fly ash in Colombia while reaching the threshold values of compressive strength and slump flow values.

Acknowledgments

References

[1] Abellán, J., Fernández, J., Torres, N. and Núñez, A., Statistical optimization of ultra-high-performance glass concrete, ACI Mater. J. 117 (1), pp. 243-254, 2020. DOI: 10.14359/51720292.

[2] Abellán-García, J., Four-layer perceptron approach for strength prediction of UHPC, Constr. Build. Mater., 256, art. 119465, 2020. DOI: 10.1016/j.conbuildmat.2020.119465.

[3] Abellán-García, J., Fernández-Gómez, J. and Torres-Castellanos, N., Properties prediction of environmentally friendly ultra-high-performance concrete using artificial neural networks, Eur. J. Environ. Civ. Eng., 0(0), pp. 1-25, 2020. DOI: 10.1080/19648189.2020.1762749.

[4] Abellan, J., Torres, N., Núñez, A. y Fernández, J., Influencia del exponente de Fuller, la relación agua conglomerante y el contenido en policarboxilato en concretos de muy altas prestaciones, en: IV Congr. Int. Ing. Civ., Havana, Cuba, 2018.

[5] Abellán, J., Fernández, J., Torres, N. and Núñez, A., Development of cost-efficient UHPC with local materials in Colombia, in: Proc. Hipermat 2020 - 5th Int. Symp. UHPC Nanotechnol. Constr. Mater., Kassel, Germany, pp. 97-98, 2020.

[6] De Larrard, F. and Sedran, T., Mixture-proportioning of high-performance concrete, Cem. Concr. Res., 32(11), pp.1699-1704, 2002. DOI: 10.1016/S0008-8846(02)00861-X.

[7] Abellán-García, J., Fernández-Gómez, J.A., Torres-Castellanos, N. and Núñez-López, A.M., Machine Learning prediction of flexural behavior of UHPFRC, in: Serna, P., Llano-Torre, A., Martí-Vargas, J.R. and Navarro-Gregori, J., (Eds.), Fibre Reinf. Concr. Improv. Innov. BEFIB 2020., RILEM Bookseries, Valencia, Spain, 2020, pp. 570-583. DOI: 10.1007/978-3-030-58482-5_52.

[8] Nehdi, M., Abbas, S. and Soliman, A., Exploratory study of ultra-high performance fiber reinforced concrete tunnel lining segments with varying steel fiber lengths and dosages, Eng. Struct. 101, pp. 733-742, 2015. DOI: 10.1016/j.engstruct.2015.07.012.

[9] Abellan, J., Torres, N., Núñez, A. and Fernández, J., Ultra high preformance fiber reinforced concrete: state of the art, applications and possibilities into the latin american market, in: XXXVIII Jornadas Sudam. Ing. Estructural, Lima, Peru, 2018.

[10] Tayeh, B.A., Abu Bakar, B.H., Megat-Johari, M.A. and Voo, Y.L., Utilization of ultra-high performance fibre concrete (UHPFC) for rehabilitation - A review, Procedia Eng. 54 (December), pp. 525-538, 2013. DOI: 10.1016/j.proeng.2013.03.048.

[11] Abellán-García, J., Nuñez-Lopez, A. and Arango-Campo, S., Pedestrian bridge over Las Vegas Avenue in Medellín. First Latin American Infrastructure in UHPFRC, in: Serna, P., Llano-Torre, A., Martí-Vargas, J.R. and Navarro-Gregori J., (Eds.), BEFIB 2020, RILEM Bookseries, Valencia (Spain), 2020, pp. 864-872. DOI: 10.1007/978-3-030-58482-5_76.

[12] Abellán, J., Núñez, A. and Arango, S., Pedestrian bridge of UNAL in Manizales : a new UPHFRC application in the Colombian building market, in: Proc. Hipermat 2020 - 5th Int. Symp. UHPC Nanotechnol. Constr. Mater., Kassel, Germany, 2020, pp. 43-44.

[13] Abdulkareem, O.M., Ben-Fraj, A., Bouasker, M. and Khelidj, A., Effect of chemical and thermal activation on the microstructural and mechanical properties of more sustainable UHPC, Constr. Build. Mater. 169, pp. 567-577, 2018. DOI: 10.1016/j.conbuildmat.2018.02.214.

[14] Richard, P. and Cheyrezy, M., Composition of reactive powder concretes, Cem. Concr. Res. 25(7), pp. 1501-1511, 1995. DOI: 10.1016/0008-8846(95)00144-2.

[15] Tuan, N.-Van, Ye, G., Breugel, K.-Van, Fraaij, A.L.A. and Danh, B., The study of using rice husk ash to produce ultra-high-performance concrete, Constr. Build. Mater., 25(4), pp. 2030-2035, 2011. DOI: 10.1016/j.conbuildmat.2010.11.046.

[16] Yu, R., Spiesz, P. and Brouwers, H.J.H., Mix design and properties assessment of Ultra-High Performance Fibre Reinforced Concrete (UHPFRC), Cem. Concr. Res., 56, pp. 29-39, 2014. DOI: 10.1016/j.cemconres.2013.11.002.

[17] Abbas, S., Nehdi, M.L. and Saleem, M.A., Ultra-High-Performance Concrete: mechanical performance, durability, sustainability and implementation challenges, Int. J. Concr. Struct. Mater. 10(3), pp. 271-295, 2016. DOI: 10.1007/s40069-016-0157-4.

[18] Shi, C., Wu, Z., Xiao, J., Wang, D., Huang, Z. and Fang, Z., A review on ultra-high-performance concrete: Part II. Hydration, microstructure and properties, Constr. Build. Mater. 101(October), pp. 741-751, 2015. DOI: 10.1016/j.conbuildmat.2015.10.088.

[19] Hisdal, J. and Bohnsdalen-Eide, M., Ultra High Performance Fibre Reinforced Concrete (UHPFRC) - State of the art, 2012.

[20] ASTM, ASTM C 618: Standard specification for coal fly ash and raw or calcined natural pozzolan for use in concrete. Annual Book of ASTM Standards, Volume 4.01, Cement; Lime; Gypsum, Annu. B. ASTM Stand, 2010, pp. 1-6. DOI: 10.1520/C0618.

[21] Malhotra, V.M. and Mehta., P.K., High-Perfomance, High-Volume Fly-Ash Concrete: materials, mixture, proportioning, properties, construction practice and case histories., 2002.

[22] Yazici, H., Yiğiter, H., Karabulut, A.Ş. and Baradan, B., Utilization of fly ash and ground granulated blast furnace slag as an alternative silica source in reactive powder concrete, Fuel., 87(12), pp. 2401-2407, 2008. DOI: 10.1016/j.fuel.2008.03.005.

[23] Ferdosian, I., Camões, A. and Ribeiro, M., High-volume fly ash paste for developing ultra-high-performance concrete (UHPC), Cienc. e Tecnol. Dos Mater., 29(1), pp. 157-161, 2016. DOI: 10.1016/j.ctmat.2016.10.001.

[24] Chen, T., Gao, X. and Ren, M., Effects of autoclave curing and fly ash on mechanical properties of ultra-high-performance concrete, Constr. Build. Mater., 158(January), pp. 864-872, 2018. DOI: 10.1016/j.conbuildmat.2017.10.074.

[25] Funk, J.E. and Dinger, D.R., Predictive process control of crowded particulate suspensions. Applied to Ceramic Manufacturing, Springer Science, New York, USA, 1994. DOI: 10.1007/978-1-4615-3118-0.

[26] Ghafari, E., Costa, H., Nuno, E. and Santos, B., RSM-based model to predict the performance of self-compacting UHPC reinforced with hybrid steel micro-fibers, Constr. Build. Mater. 66(September), pp. 375-383, 2014. DOI: 10.1016/j.conbuildmat.2014.05.064.

[27] Upasani, R.S. and Banga, A.K., Response surface methodology to investigate the iontophoretic delivery of tacrine hydrochloride, Pharm. Res., 21(12), pp.2293-2299, 2004.

[28] Lenth, R.V, Response-surface methods in R, using rsm, J. Stat. Softw., 32(7), pp. 1-17, 2012. DOI: /10.18637/jss.v032.i07.

[29] Montgomery, D.C., Design and analysis of experiments, John Wiley & Sons, Inc, New Jersey, USA, 2005.

[30] Abellan-Garcia, J., Santofimo-Vargas, M.A. and Torres-Castellanos, N., Analysis of metakaolin as partial substitution of ordinary Portland cement in Reactive Powder Concrete, Adv. Civ. Eng. Mater., 9(1), pp. 368-386, 2020. DOI: 10.1520/ACEM20190224.

[31] Roth, T., Working with the quality Tools package, [online]. 2016. Available at: http://www.r-qualitytools.org.

[32] Fonseca-Barrera, L.A., Empleo de ceniza volante colombiana como material cementicio suplementario y sus efectos sobre la fijación de cloruros en concretos, [online] 2016. Available at: http://www.bdigital.unal.edu.co/53975/.

[33] Valderrama, C.P., Torres-Agredo, J. and de Gutierrez, R., A high unburned carbon fly ash concrete's performance characteristics, Ing. e Investig. [online]. 31(1), pp. 39-46, 2011. Available at: https://www.scopus.com/inward/record.uri?eid=2-s2.0-79956129934&partnerID=40&md5=646563ee1c827e874087f000d767bf74.

[34] Kumar, R. and Tiwari, O.P., Experimental investigation of mechanical characterization and drilling of fabricated GFRP composites reinforced with Al2O3 micro particles, Int. J. Adv. Res. Ideas Innov. Technol. 4(4), pp. 191-199, 2018.

[35] ASTM, ASTM C1437, Standard test method for flow of hydraulic cement mortar, Am. Soc. Test. Mater. C-1437, 2016, pp. 1-2. DOI: 10.1520/C1437-15.2.

[36] ASTM, Standard test method for compressive strength of hydraulic cement mortars (Using 2-in . or [50-mm] Cube Specimens), Am. Soc. Test. Mater. C-109/C109M., 2010, pp. 1-9. DOI: 10.1520/C0109.

[37] R Core Team, R: a language and environment for statistical computing, Vienna, Austria, [online]. 2018. Available at: https://www.r-project.org/.

[38] The European Project Group, The european guidelines for self-compacting concrete, Eur. Guidel. Self Compact. Concrete, 2005.

[39] Ahmad, S., Hakeem, I. and Maslehuddin, M., Development of UHPC mixtures utilizing natural and industrial waste materials as partial replacements of silica fume and sand, Eur. J. Environ. Civ. Eng., (9), pp. 1106-1126, 2014. DOI: 10.1155/2014/713531.

[40] Poon, C.S., Lam, L., Kou, S.C., Wong, Y.L. and Wong, R., Rate of pozzolanic reaction of metakaolin in high-performance cement pastes, Cem. Concr. Res., 31(9), pp. 1301-1306, 2001. DOI: 10.1016/S0008-8846(01)00581-6.

[41] Ghafari, E., Costa, H. and Júlio, E., Statistical mixture design approach for eco- efficient UHPC, Cem. Concr. Compos., 55(September), pp. 17-25, 2015. DOI: 10.1016/j.cemconcomp.2014.07.016.

[42] Derringer, G. and Suich, R., Simultaneous optimization of several response variables, J. Qual. Technol., 21(4), pp. 214-219, 1980.

[43] Yan, P.Y. and Feng, J.W., Mechanical behaviour of UHPC and UHPC filled steel tubular stub columns, in: Fehling, E., Schmidt, M. and Stüwald, S. (Eds.), Proc. Int. Symp. Ultra High Perform. Concr. Second Int. Symp., University of Kassel, Germany, Kassel, Germany, 2008, pp. 355-364.

[44] Heinz, D., Urbonas, L. and Gerlicher, T., Effect of heat treatment method on the properties of UHPC, in: 3rd Int. Symp. UHPC Nanotechnol. Constr. Mater., Kassel Uni, Kassel, Germany, pp. 283-290, 2012.

[45] Huang, W., Kamezi-Kamyab, H.K., Sun, W. and Guo, L., Study on the Hydration and micro structural Development of Ultra-High-Performance Concrete with two kinds of fly ash, in: Fehling, E., Middendorf, B. and Thiemicke, J., (Eds.), Proc. Hipermat 2016 - 4th Int. Symp. UHPC Nanotechnol. Constr. Mater., University of Kassel, Germany, Kassel, Germany, 2016, pp. 22-24.

J. Abellán-Garcia, is a PhD. (c) of the Department of Civil Engineering at the Polytechnic University of Madrid (UPM), Madrid, Spain. He received a BSc. Eng. in Civil Engineering in 2006 from the Polytechnic University of Valencia (UPV) Spain, a MSc. in Railway Infrastructures, in 2010 from the Polytechnic University of Catalonia (UPC) Spain. He is also professor of civil engineering at Escuela Colombiana de Ingeniería Julio Garavito, Bogotá, Colombia. His research interests include mathematical optimization of eco-friendly ultra-high-performance concrete and seismic behavior of high strain hardening cementitious composites.
ORCID: 0000-0002-0353-322X

N. Torres-Castellanos, is a BSc. Eng. Civil Engineering from the Universidad Francisco de Paula, Santander, Colombia. MSc. in Structural Engineering from the Universidad Nacional de Colombia and PhD. in Engineering from Universidad Nacional de Colombia. Is professor of civil engineering at Escuela Colombiana de Ingeniería Julio Garavito, Bogotá, Colombia.
ORCID: 0000-0003-3293-5444

J. Fernández-Gómez, received his BSc. Eng. in Civil Engineering and PhD. in Civil Engineering from the Polytechnic University of Madrid (UPM), Madrid, Spain. Is a professor in the Department of Civil Engineering, Construction at the Polytechnic University of Madrid (UPM), Madrid, Spain. His research interests include structural analysis, construction engineering, and civil engineering materials.
ORCID: 0000-0001-9894-4357

A. Núñez-López, received his BSc. Eng. in Civil Engineering from the Universidad del Quindío, Colombia; his MSc. from the Polytechnic University of Valencia, Spain, and his PhD. in Civil Engineering from the Polytechnic University of Valencia, Spain. Is a Civil Engineer at Cementos Argos SA, Medellín, Colombia.

ORCID: 0000-0001-5811-4818